

Bending moduli for thirty-two select atomic monolayers from first principles

Shashikant Kumar and Phanish Suryanarayana*

College of Engineering, Georgia Institute of Technology, Atlanta, GA 30332, USA

E-mail: phanish.suryanarayana@ce.gatech.edu

Abstract

We calculate bending moduli along the principal directions for thirty-two select atomic monolayers using ab initio Density Functional Theory (DFT). Specifically, considering representative materials from each of Groups IV, V, III-V monolayers, transition metal dichalcogenides, Group III monochalcogenides, Group IV monochalcogenides, and transition metal trichalcogenides, we utilize the recently developed Cyclic DFT method to calculate the bending moduli in the practically relevant but previously intractable low-curvature limit. We find that the moduli generally increase with thickness of the monolayer and that structures with a rectangular lattice are prone to a higher degree of anisotropy relative to those with a honeycomb lattice. We also find that exceptions to these trends are generally a consequence of unusually strong/weak bonding and/or significant structural relaxation related effects.

Keywords

Bending modulus, Two-dimensional materials, Atomic monolayers, Density Functional Theory, Mechanical deformation, Curvature

The experimental discovery of graphene nearly two decades ago¹ has had a revolutionary effect on the field of two-dimensional materials, with dozens of atomic monolayers having now been synthesized²⁻⁶ and the potential for thousands more as predicted by ab initio calculations.^{7,8} These materials have been the subject of intensive research,⁹⁻¹¹ inspired by their exciting and fascinating properties that are typically muted or non-existent in traditional bulk counterparts, including unprecedented mechanical strength,² rare p-type electronic behavior,³ negative Poisson ratio,⁵ large piezoelectric effect,¹² topological superconductivity,¹³ high electron mobility in combination with direct band gap,⁶ and high chemical as well as thermal stability.¹⁴ Such properties make atomic monolayers ideally suited for a number of technological applications, including flexible electronics,¹⁵⁻¹⁸ nanoelectromechanical devices,¹⁹⁻²² and nanocomposites,^{23,24} wherein behavior under bending deformations is particularly important.²⁵ However, accurate estimates of a property as fundamental as even the bending modulus is not well established for these materials, providing the motivation for the current work.

Experimental data for the bending moduli of atomic monolayers is extremely sparse, likely due to the challenges associated with the experimental setup as well as the high accuracy required in measurements.²⁶ In fact, to the best of our knowledge, only the moduli of graphene^{25,27,28} have been reported to date, that too with significant error bars. In terms of computations, widely used ab initio methods like Density Functional Theory (DFT)^{29,30} provide an avenue for the accurate calculation of such material properties.³¹⁻³⁴ However, the large computational cost associated with DFT and its cubic scaling with system size restricts the calculations to curvatures that are significantly larger than those typically encountered in practice.^{25,35} A more efficient but less accurate alternative is to employ atomistic force field simulations.³⁶⁻⁴⁴ However, the resolution they provide is insufficient for the study of nanoscale systems, particularly in the presence of complex bonding. This is evident by the significant scatter in bending moduli for even elemental monolayers, with values for graphene ranging from 0.8 to 2.7 eV^{36,43} and for silicene from 0.4 to 38 eV.^{40,44}

Cyclic DFT^{35,45} is a recent ab initio method that tremendously reduces the simulation cost for systems with cyclic symmetry. In particular, by utilizing the connection between uniform bending deformations and cyclic symmetry, the method enables the calculation of bending moduli for nanostructures in the practically relevant but previously intractable low-curvature limit. In this approach, shown schematically in Fig. 1, a uniform bending deformation is applied to the nanostructure's unit cell, which is then mapped periodically in the angular direction. The cyclic symmetry of the resultant structure is then exploited to perform highly efficient DFT calculations for the ground state energy. Having done so for different deformations, the bending modulus is determined from the energy's dependence on curvature. Note that this approach neglects edge-related effects in the bending direction, justified by the nearsightedness of matter⁴⁶ and Saint-Venant's principle⁴⁷ at the electronic and continuum scales, respectively. Such assumptions are inherent to ab initio calculations for bulk properties, e.g., surface effects are neglected in Young's modulus calculations.⁴⁸

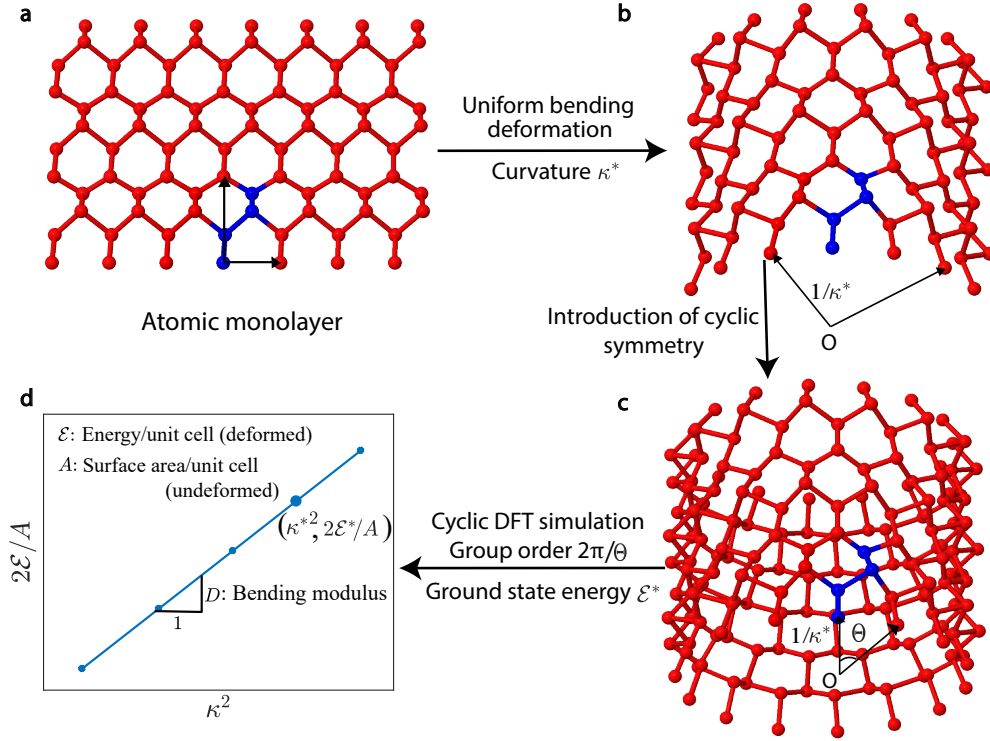


Figure 1: Schematic illustrating the calculation of bending moduli for atomic monolayers using the ab initio Cyclic DFT method. The atoms in the unit cell are colored blue.

In this work, we use the first principles Cyclic DFT method as implemented in the state of the art code SPARC-X—most recent and highly optimized version of the real-space DFT code SPARC^{49–51}—to calculate bending moduli along the principal directions for thirty-two select atomic monolayers. Specifically, we consider representative materials with honeycomb lattice structure from each of Groups IV, V, III-V monolayers, transition metal dichalcogenides (TMDs), and Group III monochalcogenides, as well as materials with rectangular lattice structure from each of Group V monolayers, Group IV monochalcogenides, and transition metal trichalcogenides (TMTs). These groups have been selected because of the significant success in the synthesis of affiliated monolayers, which are found also to demonstrate exotic and novel properties.^{1–6,52} Note that the accuracy of the Cyclic DFT formulation and implementation has been systematically and thoroughly benchmarked against established planewave⁵³ and real-space^{50,51} codes, with representative results recently published in literature,³⁵ substantiating the validity of the computations performed here.

In all simulations, we employ the PBE⁵⁴ variant of the GGA exchange-correlation functional and ONCV⁵⁵ pseudopotentials from the SG15⁵⁶ collection. All numerical parameters including grid spacing, number of points for Brillouin zone integration, vacuum in the radial direction, and structural relaxation tolerances (both cell and atom) are chosen such that the computed bending moduli are accurate to within 1%. In order to arrive at values for mildly bent sheets, i.e., corresponding to the low curvature limit, we choose curvatures in the range $0.12 \leq \kappa \leq 0.24 \text{ nm}^{-1}$, commensurate with those found in experiments.²⁵ At these curvatures, the desired precision in bending modulus translates to the ground state energy being converged to within 10^{-5} Ha/atom, necessary to capture the extremely small energy differences. Note that these highly converged large-scale DFT calculations are prohibitively expensive even with state of the art codes^{51,57,58} on the largest supercomputers. For example, the ZrTe_3 system with $\kappa = 0.16 \text{ nm}^{-1}$ has a total of 12,120 electrons and 25 **k**-points, making it intractable to traditional DFT implementations.

We first determine the suitability of the chosen exchange-correlation functional and pseu-

dopotentials for the thirty-two atomic monolayers being studied here. Specifically, starting from the structures mentioned in Table 1, which are illustrated in Fig 2, we calculate the equilibrium geometry for the monolayers using the planewave DFT code ABINIT.⁵³ The relaxed structures so obtained, details of which are presented in the Supporting Information, are found to be in very good agreement with previous theoretical predictions as well as experimental measurements.^{1-6,8,52} Having thus verified the fidelity of the DFT simulations, we now calculate the bending moduli for the monolayers along their principal directions using the aforescribed Cyclic DFT methodology. We present the results so obtained in Table 1, where D_1 and D_2 are used to denote the bending moduli along the principal directions x_1 and x_2 , respectively. The orientation of these directions relative to the different structures can be seen in Fig. 2. Indeed, for materials with a honeycomb lattice, the x_1 and x_2 directions correspond to the zigzag and armchair directions, respectively. Note that the bending moduli have been normalized with the surface area of the flat monolayer, as is typical while reporting values for two-dimensional materials.

Table 1: Bending moduli along principal directions for the thirty-two select atomic monolayers from first principles.

Group	Material	Bending moduli (eV)		Group	Material	Bending moduli (eV)	
		D_1	D_2			D_1	D_2
Groups IV, V, III-V monolayers (h1)	Si	0.36	0.37	Group III monochalcogenides (h3)	GaTe	14.9	14.5
	P	0.71	0.72		GaSe	24.1	18.9
	BN	0.56	0.58		GaS	21.2	21.7
	C	1.51	1.50		InSe	17.5	15.3
Transition metal dichalcogenides (h2)	ZrS ₂	0.62	0.80	Group V monolayers (t1)	Bi	3.55	1.05
	ZrSe ₂	2.07	2.10		Sb	3.95	1.14
	ZrTe ₂	2.84	2.16		As	5.70	1.44
	TiS ₂	2.62	2.47		P	7.59	1.44
	TiSe ₂	2.94	2.92	Group IV monochalcogenides (t1)	GeS	3.57	1.21
	TiTe ₂	4.45	4.83		GeSe	3.91	1.35
	MoS ₂	9.12	8.98		SnS	4.26	2.27
	MoSe ₂	9.07	9.21		SnSe	4.23	2.24
	WS ₂	10.3	10.1	Transition metal trichalcogenides (t2)	ZrS ₃	23.0	26.5
	WSe ₂	11.4	11.1		TiS ₃	30.4	28.5
	MoTe ₂	11.4	11.0		ZrSe ₃	33.6	27.5
	WTe ₂	12.8	12.7		ZrTe ₃	24.5	76.2

The bending moduli presented here are in reasonably good agreement with previous such ab initio DFT studies. Specifically, the bending modulus of graphene has previously been reported to be 1.46 eV,³¹ which is in good agreement with the value of ~ 1.5 eV here.¹ The same study has reported the bending modulus of BN to be 1.29 eV,³¹ which differs from the value here by ~ 0.72 eV. In the case of TMDs, the bending moduli values reported recently³³ differ by a maximum of ~ 1.07 eV from those here, while having very good qualitative agreement in the variations between the different monolayers. The quantitative differences between current work and literature can be attributed to the combined effect of a number of factors, including the accuracy of the calculations, choice of bending curvatures, and the nature of structural relaxation performed. Note that though there are a few other works which calculate the bending moduli of atomic monolayers using DFT,^{32,34,35} here we have only explicitly compared against those that employ the same exchange-correlation functional, i.e., PBE, since values can vary based on this choice.

We observe from the results that the bending moduli span nearly three orders of magnitude between the different monolayers, silicene being at one end of the spectrum with ~ 0.36 eV and ZrTe₃ at the other end with ~ 76.2 eV. Graphene is towards the lower end, being only a few fold larger than silicene and more than an order of magnitude smaller than ZrTe₃. In terms of groups, Group III monochalcogenides and TMTs have the largest bending moduli among structures with honeycomb and rectangular lattices, respectively. Specifically, the values for both these groups are similar, with TMTs having larger moduli overall. We also observe from the results that, apart from TMTs, groups with a rectangular lattice have a higher degree of anisotropy compared to those with a honeycomb lattice. Specifically, while the bending moduli of honeycomb structures are generally similar in the armchair and zigzag directions, rectangular structures have up to a five-fold difference in the values along the principal directions. This trend is epitomized by phosphorene, which demonstrates significant anisotropy in the rectangular but not honeycomb lattice configurations.

¹The computed bending modulus for graphene is also in good agreement with recent experimental measurements,²⁷ where the value is reported to be in the range 1.2 to 1.7 eV.

The above observations regarding the variation in bending moduli between the different monolayers as well as the different directions within monolayers merit further discussion. Since the exact values are determined by the complex interplay between structure, composition, and electronic structure effects, here we focus on general trends. If the monolayers are modeled as plates in the spirit of traditional continuum mechanics,⁵⁹ then the bending moduli are expected to scale cubically with the thickness. Though the exact value of thickness for monolayers like graphene is controversial,⁶⁰ in the current context we correlate it with the spatial extent of the electron density in DFT. However, such a continuum formulation neglects the highly inhomogeneous nature of the bonding that can occur in atomic monolayers, rendering the scaling laws unrepresentative for these systems, a conclusion that is indeed supported by the data here. It is nevertheless true that in the absence of structural relaxation, there is larger distortion in the bonding along the bending direction as one moves away from the center of the monolayer (i.e., neutral axis). This translates to increase in bending moduli with monolayer thickness, exceptions being materials that have unusually strong (e.g. graphene and BN^{61,62}) or weak (e.g. TiS₂ and TiTe₂) bonding, and/or those with significant structural relaxation related effects (e.g., TMTs, as discussed below).²

In view of the above discussion, we plot in Fig. 2 contours of electron density difference between the flat and bent monolayers for silicene, WSe₂, GaTe, phosphorene, and ZrS₃: materials with varied structure that have bending moduli spanning the range of values reported here. The contours are plotted in the undeformed configuration and on the x_1x_2 -plane passing through the furthest atom from the monolayer center. It is clear that the electron density perturbations generally increase with monolayer thickness, resulting in the bending moduli following a similar trend. In addition, there is noticeable difference in the electron density perturbations between the two bending directions for phosphorene, leading to its significant anisotropy. Similar to previous conclusions for various properties,^{63–66} this can be attributed to the lower degree of structural symmetry in rectangular lattices. Note that TMTs are

²The bending moduli values in the absence of structural relaxation can be found in the Supporting Information.

exceptions to these trends, as evident from the contours for ZrS_3 , wherein the electron density perturbations are similar for both bending directions. We have found that this is a consequence of structural relaxation related effects: there is a drastic drop in the value of D_2 for TMTs, e.g., the value for TiS_3 drops from 87.4 to 28.5 eV and the value for ZrS_3 drops from 82.6 to 26.5 eV. In particular, we have found that the distance between the two atoms furthest from the neutral axis is significantly reduced after relaxation, taking a value similar to that obtained for bending along the x_1 direction, both of which are close to the distance in the flat sheet. This essentially negates the effect of the bending deformation in the region where it is expected to have the maximum effect, thereby resulting in the drastic reductions. Note that the significant anisotropy observed for honeycomb structured ZrS_2 and GaSe can similarly be explained in terms of structural relaxation related effects, as evident from the unrelaxed bending moduli values presented in the Supporting Information.

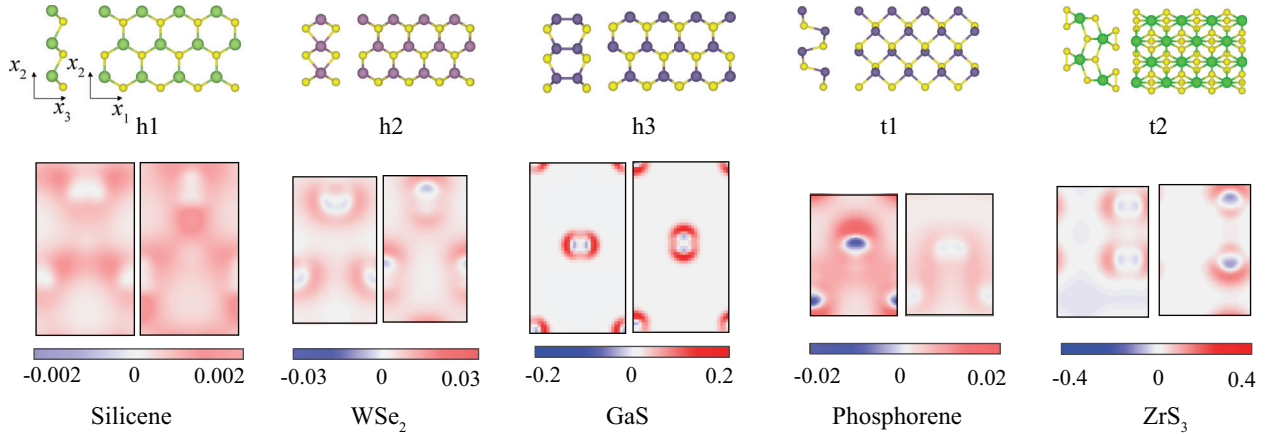


Figure 2: Contours of electron density difference between the flat and bent ($\kappa \sim 0.2 \text{ nm}^{-1}$) atomic monolayers. The contours are in the undeformed configuration and on the x_1x_2 -plane passing through the furthest atom from the monolayer center, with the figures to the left and right for each material corresponding to bending along the x_1 and x_2 directions, respectively.

In summary, we have calculated bending moduli along the principal directions for thirty-two select atomic monolayers from first principles. In particular, we have used the recent Cyclic DFT method to calculate the bending moduli of the two-dimensional materials in the practically relevant but previously intractable low-curvature limit. We have found that

the moduli generally increase with monolayer thickness, spanning nearly three orders of magnitude between the different materials. In addition, we have found that monolayers with rectangular lattice structures are prone to a higher degree of anisotropy relative to those with honeycomb lattices. Exceptions to these trends generally result from unusually strong/weak bonding and/or significant structural relaxation related effects. Overall, this work provides an important reference for the bending moduli of a number of important atomic monolayers.

Supporting Information

Equilibrium geometries of atomic monolayers, unrelaxed bending moduli

Acknowledgments

The authors gratefully acknowledge the support of the U.S. National Science Foundation (CAREER-1553212).

References

- (1) Novoselov, K. S.; Jiang, D.; Schedin, F.; Booth, T. J.; Khotkevich, V. V.; Morozov, S. V.; Geim, A. K. Two-dimensional atomic crystals. *Proceedings of the National Academy of Sciences* **2005**, *102*, 10451–10453.
- (2) Balendhran, S.; Walia, S.; Nili, H.; Sriram, S.; Bhaskaran, M. Elemental analogues of graphene: silicene, germanene, stanene, and phosphorene. *Small* **2015**, *11*, 640–652.
- (3) Zhou, S.; Liu, C.-C.; Zhao, J.; Yao, Y. Monolayer group-III monochalcogenides by oxygen functionalization: a promising class of two-dimensional topological insulators. *npj Quantum Materials* **2018**, *3*, 1–7.

- (4) Vaughn, D. D.; Patel, R. J.; Hickner, M. A.; Schaak, R. E. Single-crystal colloidal nanosheets of GeS and GeSe. *Journal of the American Chemical Society* **2010**, *132*, 15170–15172.
- (5) Zhang, S.; Guo, S.; Chen, Z.; Wang, Y.; Gao, H.; Gómez-Herrero, J.; Ares, P.; Zamora, F.; Zhu, Z.; Zeng, H. Recent progress in 2D group-VA semiconductors: from theory to experiment. *Chemical Society Reviews* **2018**, *47*, 982–1021.
- (6) Dai, J.; Li, M.; Zeng, X. C. Group IVB transition metal trichalcogenides: a new class of 2D layered materials beyond graphene. *Wiley Interdisciplinary Reviews: Computational Molecular Science* **2016**, *6*, 211–222.
- (7) Hastrup, S.; Strange, M.; Pandey, M.; Deilmann, T.; Schmidt, P. S.; Hinsche, N. F.; Gjerding, M. N.; Torelli, D.; Larsen, P. M.; Riis-Jensen, A. C.; Gath, J.; Jacobsen, K. W.; Mortensen, J. J.; Olsen, T.; Thygesen, K. S. The Computational 2D Materials Database: high-throughput modeling and discovery of atomically thin crystals. *2D Materials* **2018**, *5*, 042002.
- (8) Zhou, J.; Shen, L.; Costa, M. D.; Persson, K. A.; Ong, S. P.; Huck, P.; Lu, Y.; Ma, X.; Chen, Y.; Tang, H.; Feng, Y. P. 2DMatPedia, an open computational database of two-dimensional materials from top-down and bottom-up approaches. *Scientific data* **2019**, *6*, 1–10.
- (9) Mas-Balleste, R.; Gomez-Navarro, C.; Gomez-Herrero, J.; Zamora, F. 2D materials: to graphene and beyond. *Nanoscale* **2011**, *3*, 20–30.
- (10) Butler, S. Z. et al. Progress, Challenges, and Opportunities in Two-Dimensional Materials Beyond Graphene. *ACS Nano* **2013**, *7*, 2898–2926.
- (11) Geng, D.; Yang, H. Y. Recent advances in growth of novel 2D materials: beyond graphene and transition metal dichalcogenides. *Advanced Materials* **2018**, *30*, 1800865.

- (12) Fei, R.; Li, W.; Li, J.; Yang, L. Giant piezoelectricity of monolayer group IV monochalcogenides: SnSe, SnS, GeSe, and GeS. *Applied Physics Letters* **2015**, *107*, 173104.
- (13) Hsu, Y.-T.; Vaezi, A.; Fischer, M. H.; Kim, E.-A. Topological superconductivity in monolayer transition metal dichalcogenides. *Nature communications* **2017**, *8*, 1–6.
- (14) Jiang, X.-F.; Weng, Q.; Wang, X.-B.; Li, X.; Zhang, J.; Golberg, D.; Bando, Y. Recent progress on fabrications and applications of boron nitride nanomaterials: a review. *Journal of Materials Science & Technology* **2015**, *31*, 589–598.
- (15) Pu, J.; Yomogida, Y.; Liu, K.-K.; Li, L.-J.; Iwasa, Y.; Takenobu, T. Highly flexible MoS₂ thin-film transistors with ion gel dielectrics. *Nano Letters* **2012**, *12*, 4013–4017.
- (16) Lee, G.-H.; Yu, Y.-J.; Cui, X.; Petrone, N.; Lee, C.-H.; Choi, M. S.; Lee, D.-Y.; Lee, C.; Yoo, W. J.; Watanabe, K.; Taniguchi, T.; Nuckolls, C.; Kim, P.; Hone, J. Flexible and transparent MoS₂ field-effect transistors on hexagonal boron nitride-graphene heterostructures. *ACS Nano* **2013**, *7*, 7931–7936.
- (17) Salvatore, G. A.; Munzenrieder, N.; Barraud, C.; Petti, L.; Zysset, C.; Buthe, L.; Ensslin, K.; Troster, G. Fabrication and transfer of flexible few-layers MoS₂ thin film transistors to any arbitrary substrate. *ACS Nano* **2013**, *7*, 8809–8815.
- (18) Yoon, J.; Park, W.; Bae, G.-Y.; Kim, Y.; SooJang, H.; Hyun, Y.; Lim, S. K.; Kahng, Y. H.; Hong, W.-K.; Lee, B. H.; Ko, H. C. Highly flexible and transparent multilayer MoS₂ transistors with graphene electrodes. *Small* **2013**, *9*, 3295–3300.
- (19) Zhang, Y.; Zheng, B.; Zhu, C.; Zhang, X.; Tan, C.; Li, H.; Chen, B.; Yang, J.; Chen, J.; Huang, Y.; Wang, L.; Zhang, H. Single-layer transition metal dichalcogenide nanosheet-based nanosensors for rapid, sensitive, and multiplexed detection of DNA. *Advanced Materials* **2015**, *27*, 935–939.

- (20) Sakhaee-Pour, A.; Ahmadian, M.; Vafai, A. Potential application of single-layered graphene sheet as strain sensor. *Solid State Communications* **2008**, *147*, 336–340.
- (21) Sazonova, V.; Yaish, Y.; Üstünel, H.; Roundy, D.; Arias, T. A.; McEuen, P. L. A tunable carbon nanotube electromechanical oscillator. *Nature* **2004**, *431*, 284.
- (22) Bunch, J. S.; Zande, A. M. V. D.; Verbridge, S. S.; Frank, I. W.; Tanenbaum, D. M.; Parpia, J. M.; Craighead, H. G.; McEuen, P. L. Electromechanical resonators from graphene sheets. *Science* **2007**, *315*, 490–493.
- (23) Novoselov, K.; Neto, A. C. Two-dimensional crystals-based heterostructures: materials with tailored properties. *Physica Scripta* **2012**, *2012*, 014006.
- (24) Qin, Y.; Peng, Q.; Ding, Y.; Lin, Z.; Wang, C.; Li, Y.; Xu, F.; Li, J.; Yuan, Y.; He, X.; Li, Y. Lightweight, superelastic, and mechanically flexible graphene/polyimide nanocomposite foam for strain sensor application. *ACS Nano* **2015**, *9*, 8933–8941.
- (25) Lindahl, N.; Midtvedt, D.; Svensson, J.; Nerushev, O. A.; Lindvall, N.; Isacson, A.; Campbell, E. E. Determination of the bending rigidity of graphene via electrostatic actuation of buckled membranes. *Nano Letters* **2012**, *12*, 3526–3531.
- (26) Akinwande, D. et al. A review on mechanics and mechanical properties of 2D materials Graphene and beyond. *Extreme Mechanics Letters* **2017**, *13*, 42–77.
- (27) Han, E.; Yu, J.; Annevelink, E.; Son, J.; Kang, D. A.; Watanabe, K.; Taniguchi, T.; Ertekin, E.; Huang, P. Y.; van der Zande, A. M. Ultrasoft slip-mediated bending in few-layer graphene. *Nature materials* **2019**, 1–5.
- (28) Nicklow, R.; Wakabayashi, N.; Smith, H. Lattice dynamics of pyrolytic graphite. *Physical Review B* **1972**, *5*, 4951.
- (29) Hohenberg, P.; Kohn, W. Inhomogeneous Electron Gas. *Physical Review* **1964**, *136*, B864–B871.

- (30) Kohn, W.; Sham, L. J. Self-Consistent Equations Including Exchange and Correlation Effects. *Physical Review* **1965**, *140*, A1133–A1138.
- (31) Kudin, K. N.; Scuseria, G. E.; Yakobson, B. I. C₂F, BN, and C nanoshell elasticity from ab initio computations. *Physical Review B* **2001**, *64*, 235406.
- (32) Zhao, J.; Deng, Q.; Ly, T. H.; Han, G. H.; Sandeep, G.; Rummeli, M. H. Two-dimensional membrane as elastic shell with proof on the folds revealed by three-dimensional atomic mapping. *Nature communications* **2015**, *6*, 1–6.
- (33) Lai, K.; Zhang, W.-B.; Zhou, F.; Zeng, F.; Tang, B.-Y. Bending rigidity of transition metal dichalcogenide monolayers from first-principles. *Journal of Physics D: Applied Physics* **2016**, *49*, 185301.
- (34) Nepal, N. K.; Yu, L.; Yan, Q.; Ruzsinszky, A. First-principles study of mechanical and electronic properties of bent monolayer transition metal dichalcogenides. *Physical Review Materials* **2019**, *3*, 073601.
- (35) Ghosh, S.; Banerjee, A. S.; Suryanarayana, P. Symmetry-adapted real-space density functional theory for cylindrical geometries: Application to large group-IV nanotubes. *Physical Review B* **2019**, *100*, 125143.
- (36) Arroyo, M.; Belytschko, T. Finite crystal elasticity of carbon nanotubes based on the exponential Cauchy-Born rule. *Physical Review B* **2004**, *69*, 115415.
- (37) Koskinen, P.; Kit, O. O. Approximate modeling of spherical membranes. *Physical Review B* **2010**, *82*, 235420.
- (38) Cranford, S.; Sen, D.; Buehler, M. J. Meso-origami: folding multilayer graphene sheets. *Applied physics letters* **2009**, *95*, 123121.
- (39) Cranford, S.; Buehler, M. J. Twisted and coiled ultralong multilayer graphene ribbons. *Modelling and Simulation in Materials Science and Engineering* **2011**, *19*, 054003.

- (40) Roman, R. E.; Cranford, S. W. Mechanical properties of silicene. *Computational Materials Science* **2014**, *82*, 50–55.
- (41) Liu, Y.; Xu, Z.; v, Q. The interlayer shear effect on graphene multilayer resonators. *Journal of the Mechanics and Physics of Solids* **2011**, *59*, 1613–1622.
- (42) Xu, Z.; Buehler, M. J. Geometry controls conformation of graphene sheets: membranes, ribbons, and scrolls. *ACS nano* **2010**, *4*, 3869–3876.
- (43) Sajadi, B.; van Hemert, S.; Arash, B.; Belardinelli, P.; Steeneken, P. G.; Alijani, F. Size-and temperature-dependent bending rigidity of graphene using modal analysis. *Carbon* **2018**, *139*, 334–341.
- (44) Qian, C.; Li, Z. Multilayer silicene: Structure, electronics, and mechanical property. *Computational Materials Science* **2020**, *172*, 109354.
- (45) Banerjee, A. S.; Suryanarayana, P. Cyclic density functional theory: A route to the first principles simulation of bending in nanostructures. *Journal of the Mechanics and Physics of Solids* **2016**, *96*, 605–631.
- (46) Prodan, E.; Kohn, W. Nearsightedness of electronic matter. *Proceedings of the National Academy of Sciences of the United States of America* **2005**, *102*, 11635–11638.
- (47) Iesan, D. *Saint-Venant’s problem*; Springer, 2006; Vol. 1279.
- (48) Cooper, R. C.; Lee, C.; Marianetti, C. A.; Wei, X.; Hone, J.; Kysar, J. W. Nonlinear elastic behavior of two-dimensional molybdenum disulfide. *Physical Review B* **2013**, *87*, 035423.
- (49) Xu, Q.; Sharma, A.; Comer, B.; Huang, H.; Chow, E.; Medford, A. J.; Pask, J. E.; Suryanarayana, P. SPARC: Simulation Package for Ab-initio Real-space Calculations. *arXiv preprint arXiv:2005.10431* **2020**,

- (50) Ghosh, S.; Suryanarayana, P. SPARC: Accurate and efficient finite-difference formulation and parallel implementation of Density Functional Theory: Isolated clusters. *Computer Physics Communications* **2017**, *212*, 189–204.
- (51) Ghosh, S.; Suryanarayana, P. SPARC: Accurate and efficient finite-difference formulation and parallel implementation of Density Functional Theory: Extended systems. *Computer Physics Communications* **2017**, *216*, 109–125.
- (52) Coleman, J. N. et al. Two-dimensional nanosheets produced by liquid exfoliation of layered materials. *Science* **2011**, *331*, 568–571.
- (53) Gonze, X. et al. First-principles computation of material properties: the ABINIT software project. *Computational Materials Science* **2002**, *25*, 478–492(15).
- (54) Perdew, J. P.; Yue, W. Accurate and simple density functional for the electronic exchange energy: Generalized gradient approximation. *Physical Review B* **1986**, *33*, 8800.
- (55) Hamann, D. R. Optimized norm-conserving Vanderbilt pseudopotentials. *Physical Review B* **2013**, *88*, 085117.
- (56) Schlipf, M.; Gygi, F. Optimization algorithm for the generation of ONCV pseudopotentials. *Computer Physics Communications* **2015**, *196*, 36 – 44.
- (57) Banerjee, A. S.; Lin, L.; Suryanarayana, P.; Yang, C.; Pask, J. E. Two-level Chebyshev filter based complementary subspace method: pushing the envelope of large-scale electronic structure calculations. *Journal of chemical theory and computation* **2018**, *14*, 2930–2946.
- (58) Motamarri, P.; Das, S.; Rudraraju, S.; Ghosh, K.; Davydov, D.; Gavini, V. DFT-FE-A massively parallel adaptive finite-element code for large-scale density functional theory calculations. *Computer Physics Communications* **2020**, *246*, 106853.
- (59) Reddy, J. N. *Theory and analysis of elastic plates and shells*; CRC press, 2006.

- (60) Huang, Y.; Wu, J.; Hwang, K.-C. Thickness of graphene and single-wall carbon nanotubes. *Physical review B* **2006**, *74*, 245413.
- (61) Demczyk, B. G.; Wang, Y. M.; Cumings, J.; Hetman, M.; Han, W.; Zettl, A.; Ritchie, R. Direct mechanical measurement of the tensile strength and elastic modulus of multiwalled carbon nanotubes. *Materials Science and Engineering: A* **2002**, *334*, 173–178.
- (62) Wang, J.; Ma, F.; Sun, M. Graphene, hexagonal boron nitride, and their heterostructures: properties and applications. *RSC advances* **2017**, *7*, 16801–16822.
- (63) Li, L.; Han, W.; Pi, L.; Niu, P.; Han, J.; Wang, C.; Su, B.; Li, H.; Xiong, J.; Bando, Y.; Zhai, T. Emerging in-plane anisotropic two-dimensional materials. *InfoMat* **2019**, *1*, 54–73.
- (64) Xia, F.; Wang, H.; Jia, Y. Rediscovering black phosphorus as an anisotropic layered material for optoelectronics and electronics. *Nature Communications* **2014**, *5*, 1–6.
- (65) Wang, X.; Jones, A. M.; Seyler, K. L.; Tran, V.; Jia, Y.; Zhao, H.; Wang, H.; Yang, L.; Xu, X.; Xia, F. Highly anisotropic and robust excitons in monolayer black phosphorus. *Nature Nanotechnology* **2015**, *10*, 517–521.
- (66) Luo, Z.; Maassen, J.; Deng, Y.; Du, Y.; Garrelts, R. P.; Lundstrom, M. S.; Peide, D. Y.; Xu, X. Anisotropic in-plane thermal conductivity observed in few-layer black phosphorus. *Nature Communications* **2015**, *6*, 1–8.